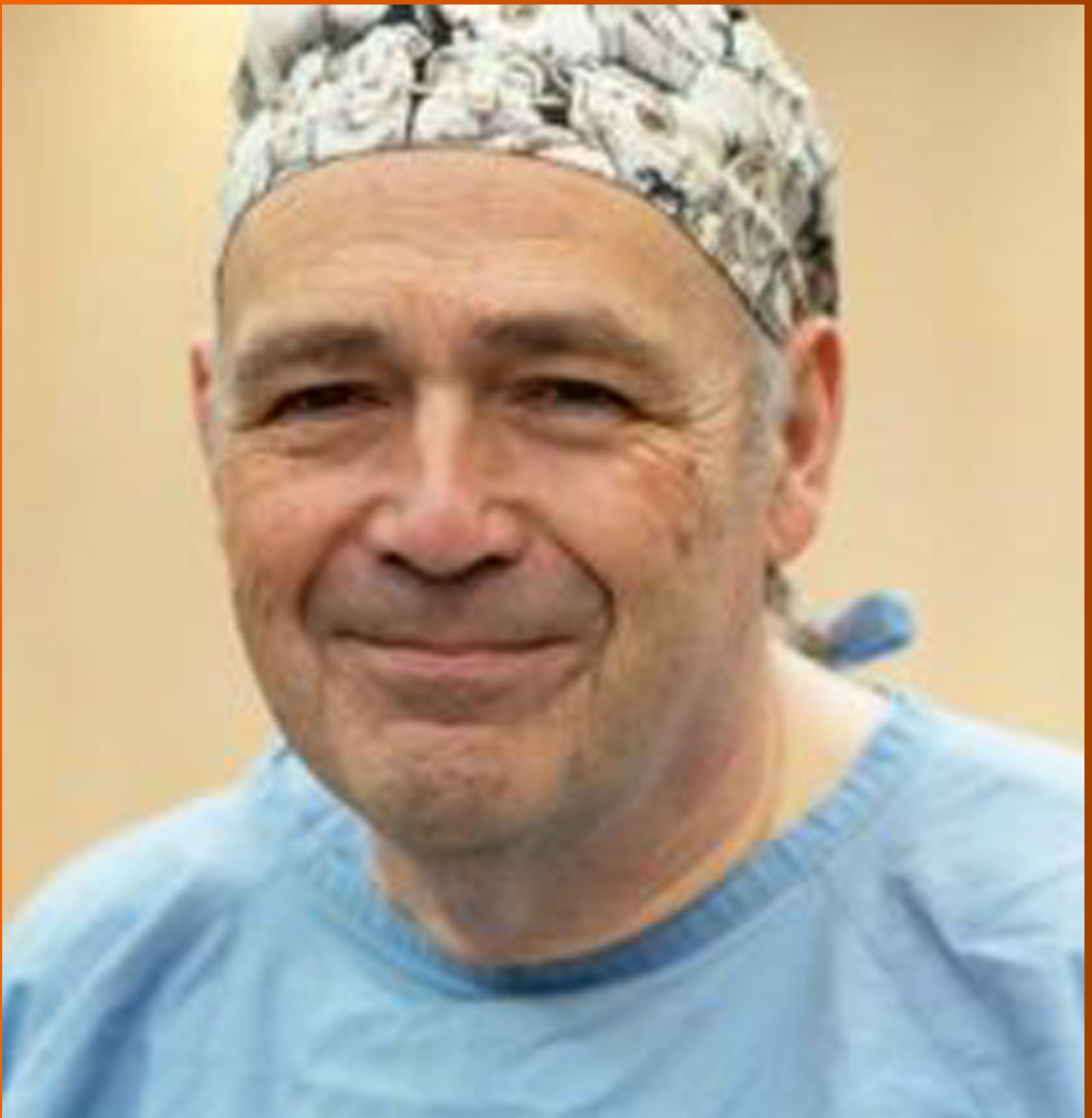


# World Journal of *Gastroenterology*

*World J Gastroenterol* 2024 March 21; 30(11): 1470-1643



**EDITORIAL**

- 1470 MicroRNAs in hepatocellular carcinoma treatment: Charting the path forward  
*Lin HT, Castaneda AFA, Krishna SG, Mumtaz K*
- 1475 Innovative pathways allow safe discharge of mild acute pancreatitis from the emergency room  
*Kothari DJ, Sheth SG*
- 1480 Current remarks and future directions on the interactions between metabolic dysfunction-associated fatty liver disease and COVID-19  
*Brilakis L, Theofilogiannakou E, Lykoudis PM*
- 1488 Routine utilization of machine perfusion in liver transplantation: Ready for prime time?  
*Parente A, Sun K, Dutkowski P, Shapiro AJ, Schlegel A*
- 1494 Advancements in Barrett's esophagus detection: The role of artificial intelligence and its implications  
*Massironi S*

**REVIEW**

- 1497 MicroRNAs: A novel signature in the metastasis of esophageal squamous cell carcinoma  
*Wei QY, Jin F, Wang ZY, Li BJ, Cao WB, Sun ZY, Mo SJ*

**MINIREVIEWS**

- 1524 Morphological and biochemical characteristics associated with autophagy in gastrointestinal diseases  
*Chang YF, Li JJ, Liu T, Wei CQ, Ma LW, Nikolenko VN, Chang WL*

**ORIGINAL ARTICLE****Retrospective Study**

- 1533 Efficacy of radiofrequency ablation combined with sorafenib for treating liver cancer complicated with portal hypertension and prognostic factors  
*Yang LM, Wang HJ, Li SL, Gan GH, Deng WW, Chang YS, Zhang LF*

**Clinical Trials Study**

- 1545 Effect of *Aspergillus niger* prolyl endopeptidase in patients with celiac disease on a long-term gluten-free diet  
*Stefanolo JP, Segura V, Grizzuti M, Heredia A, Comino I, Costa AF, Puebla R, Temprano MP, Niveloni SI, de Diego G, Oregui ME, Smecuol EG, de Marzi MC, Verdú EF, Sousa C, Bai JC*
- 1556 Effects of *Lactobacillus paracasei* N1115 on gut microbial imbalance and liver function in patients with hepatitis B-related cirrhosis  
*Hu YC, Ding XC, Liu HJ, Ma WL, Feng XY, Ma LN*

**Prospective Study**

- 1572 Washed microbiota transplantation for Crohn's disease: A metagenomic, metatranscriptomic, and metabolomic-based study  
*Chen SJ, Zhang DY, Wu X, Zhang FM, Cui BT, Huang YH, Zhang ZL, Wang R, Bai FH*

**Basic Study**

- 1588 Silent information regulator sirtuin 1 ameliorates acute liver failure *via* the p53/glutathione peroxidase 4/gasdermin D axis  
*Zhou XN, Zhang Q, Peng H, Qin YJ, Liu YH, Wang L, Cheng ML, Luo XH, Li H*
- 1609 Identification of an immune-related gene signature for predicting prognosis and immunotherapy efficacy in liver cancer *via* cell-cell communication  
*Li JT, Zhang HM, Wang W, Wei DQ*

**META-ANALYSIS**

- 1621 Effects of neoadjuvant chemotherapy *vs* chemoradiotherapy in the treatment of esophageal adenocarcinoma: A systematic review and meta-analysis  
*Csontos A, Fazekas A, Szakó L, Farkas N, Papp C, Ferenczi S, Bellyei S, Hegyi P, Papp A*

**CASE REPORT**

- 1636 Myocardial metastasis from ZEB1- and TWIST-positive spindle cell carcinoma of the esophagus: A case report  
*Shibata Y, Ohmura H, Komatsu K, Sagara K, Matsuyama A, Nakano R, Baba E*

**ABOUT COVER**

Editorial Board of *World Journal of Gastroenterology*, David L Morris, MD, FRCS (Ed), Professor, Department of Surgery, University of New South Wales, Sydney 2217, New South Wales, Australia. david.morris@unsw.edu.au

**AIMS AND SCOPE**

The primary aim of *World Journal of Gastroenterology* (*WJG*, *World J Gastroenterol*) is to provide scholars and readers from various fields of gastroenterology and hepatology with a platform to publish high-quality basic and clinical research articles and communicate their research findings online. *WJG* mainly publishes articles reporting research results and findings obtained in the field of gastroenterology and hepatology and covering a wide range of topics including gastroenterology, hepatology, gastrointestinal endoscopy, gastrointestinal surgery, gastrointestinal oncology, and pediatric gastroenterology.

**INDEXING/ABSTRACTING**

The *WJG* is now abstracted and indexed in Science Citation Index Expanded (SCIE), MEDLINE, PubMed, PubMed Central, Scopus, Reference Citation Analysis, China Science and Technology Journal Database, and Superstar Journals Database. The 2023 edition of Journal Citation Reports® cites the 2022 impact factor (IF) for *WJG* as 4.3; Quartile category: Q2. The *WJG*'s CiteScore for 2021 is 8.3.

**RESPONSIBLE EDITORS FOR THIS ISSUE**

Production Editor: Yi-Xuan Cai; Production Department Director: Xu Guo; Cover Editor: Jia-Ru Fan.

**NAME OF JOURNAL**

*World Journal of Gastroenterology*

**ISSN**

ISSN 1007-9327 (print) ISSN 2219-2840 (online)

**LAUNCH DATE**

October 1, 1995

**FREQUENCY**

Weekly

**EDITORS-IN-CHIEF**

Andrzej S Tarnawski

**EXECUTIVE ASSOCIATE EDITORS-IN-CHIEF**

Xian-Jun Yu (Pancreatic Oncology), Jian-Gao Fan (Chronic Liver Disease), Hou-Bao Liu (Biliary Tract Disease)

**EDITORIAL BOARD MEMBERS**

<http://www.wjgnet.com/1007-9327/editorialboard.htm>

**PUBLICATION DATE**

March 21, 2024

**COPYRIGHT**

© 2024 Baishideng Publishing Group Inc

**PUBLISHING PARTNER**

Shanghai Pancreatic Cancer Institute and Pancreatic Cancer Institute, Fudan University  
Biliary Tract Disease Institute, Fudan University

**INSTRUCTIONS TO AUTHORS**

<https://www.wjgnet.com/bpg/gcrinfo/204>

**GUIDELINES FOR ETHICS DOCUMENTS**

<https://www.wjgnet.com/bpg/GerInfo/287>

**GUIDELINES FOR NON-NATIVE SPEAKERS OF ENGLISH**

<https://www.wjgnet.com/bpg/gcrinfo/240>

**PUBLICATION ETHICS**

<https://www.wjgnet.com/bpg/GerInfo/288>

**PUBLICATION MISCONDUCT**

<https://www.wjgnet.com/bpg/gcrinfo/208>

**POLICY OF CO-AUTHORS**

<https://www.wjgnet.com/bpg/GerInfo/310>

**ARTICLE PROCESSING CHARGE**

<https://www.wjgnet.com/bpg/gcrinfo/242>

**STEPS FOR SUBMITTING MANUSCRIPTS**

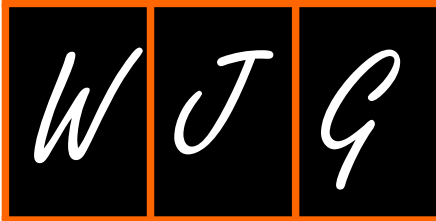
<https://www.wjgnet.com/bpg/GerInfo/239>

**ONLINE SUBMISSION**

<https://www.f6publishing.com>

**PUBLISHING PARTNER'S OFFICIAL WEBSITE**

<https://www.shca.org.cn>  
<https://www.zs-hospital.sh.cn>



Basic Study

# Identification of an immune-related gene signature for predicting prognosis and immunotherapy efficacy in liver cancer *via* cell-cell communication

Jun-Tao Li, Hong-Mei Zhang, Wei Wang, Dong-Qing Wei

**Specialty type:** Gastroenterology and hepatology

**Provenance and peer review:** Invited article; Externally peer reviewed.

**Peer-review model:** Single blind

**Peer-review report's scientific quality classification**

Grade A (Excellent): A  
Grade B (Very good): 0  
Grade C (Good): 0  
Grade D (Fair): 0  
Grade E (Poor): 0

**P-Reviewer:** Rodrigues AT, Brazil

**Received:** December 13, 2023

**Peer-review started:** December 13, 2023

**First decision:** December 27, 2023

**Revised:** January 9, 2024

**Accepted:** March 4, 2024

**Article in press:** March 4, 2024

**Published online:** March 21, 2024



**Jun-Tao Li, Hong-Mei Zhang,** College of Mathematics and Information Science, Henan Normal University, Xinxiang 453007, Henan Province, China

**Wei Wang,** College of Computer and Information Engineering, Henan Normal University, Xinxiang 453007, Henan Province, China

**Dong-Qing Wei,** State Key Laboratory of Microbial Metabolism, and School of Life Sciences and Biotechnology, Shanghai Jiao Tong University, Shanghai 200240, China

**Corresponding author:** Hong-Mei Zhang, MPhil, Master's Student, College of Mathematics and Information Science, Henan Normal University, Jianshe East Road, Xinxiang 453007, Henan Province, China. [zhanghmmail@163.com](mailto:zhanghmmail@163.com)

## Abstract

### BACKGROUND

Liver cancer is one of the deadliest malignant tumors worldwide. Immunotherapy has provided hope to patients with advanced liver cancer, but only a small fraction of patients benefit from this treatment due to individual differences. Identifying immune-related gene signatures in liver cancer patients not only aids physicians in cancer diagnosis but also offers personalized treatment strategies, thereby improving patient survival rates. Although several methods have been developed to predict the prognosis and immunotherapeutic efficacy in patients with liver cancer, the impact of cell-cell interactions in the tumor microenvironment has not been adequately considered.

### AIM

To identify immune-related gene signals for predicting liver cancer prognosis and immunotherapy efficacy.

### METHODS

Cell grouping and cell-cell communication analysis were performed on single-cell RNA-sequencing data to identify highly active cell groups in immune-related pathways. Highly active immune cells were identified by intersecting the highly active cell groups with B cells and T cells. The significantly differentially expressed genes between highly active immune cells and other cells were subsequently selected as features, and a least absolute shrinkage and selection

operator (LASSO) regression model was constructed to screen for diagnostic-related features. Fourteen genes that were selected more than 5 times in 10 LASSO regression experiments were included in a multivariable Cox regression model. Finally, 3 genes (stathmin 1, cofilin 1, and C-C chemokine ligand 5) significantly associated with survival were identified and used to construct an immune-related gene signature.

## RESULTS

The immune-related gene signature composed of stathmin 1, cofilin 1, and C-C chemokine ligand 5 was identified through cell-cell communication. The effectiveness of the identified gene signature was validated based on experimental results of predictive immunotherapy response, tumor mutation burden analysis, immune cell infiltration analysis, survival analysis, and expression analysis.

## CONCLUSION

The findings suggest that the identified gene signature may contribute to a deeper understanding of the activity patterns of immune cells in the liver tumor microenvironment, providing insights for personalized treatment strategies.

**Key Words:** Liver cancer; Cell-cell communication; Gene signature; Prognosis; Immunotherapy; Single-cell RNA sequencing

©The Author(s) 2024. Published by Baishideng Publishing Group Inc. All rights reserved.

**Core Tip:** In this study, CellChat was employed to infer cell-cell communication, thereby selecting highly active cell groups in immune-related pathways on single-cell RNA-sequencing data. Highly active immune cells were identified by intersecting these groups with B and T cells. Subsequently, significantly differentially expressed genes between highly active immune cells and the remaining cells were incorporated into the Lasso regression model. Ultimately, incorporating genes selected more than 5 times in 10 Lasso regression experiments into a multivariable Cox regression model, 3 genes (stathmin 1, cofilin 1, and C-C chemokine ligand 5) significantly associated with survival were identified to construct a gene signature.

**Citation:** Li JT, Zhang HM, Wang W, Wei DQ. Identification of an immune-related gene signature for predicting prognosis and immunotherapy efficacy in liver cancer *via* cell-cell communication. *World J Gastroenterol* 2024; 30(11): 1609-1620

**URL:** <https://www.wjgnet.com/1007-9327/full/v30/i11/1609.htm>

**DOI:** <https://dx.doi.org/10.3748/wjg.v30.i11.1609>

## INTRODUCTION

Liver cancer, a malignant tumor with consistently high global incidence and mortality rates, has long been a focal point of medical research and clinical intervention[1,2]. In particular, within the rapidly advancing field of immunotherapy, immune checkpoint blockade (ICB) treatment has emerged as an innovative therapeutic approach, offering renewed hope for patients with liver cancer[3]. This strategy has achieved significant clinical efficacy by preventing tumor cells from suppressing the immune system and stimulating the body's own immune response[3-5]. However, only a small fraction of liver cancer patients benefit from this treatment, and the molecular basis underlying the control of immune responses and evasion has not been determined[6,7]. To better guide treatment strategies and predict patient prognosis, it is imperative to explore into the molecular mechanisms and immune characteristics of liver cancer.

The success of immunotherapy in liver cancer hinges on a comprehensive understanding of the tumor immune microenvironment, necessitating the exploration of high-throughput technologies to unravel intricate molecular interactions[8-10]. Using bulk RNA sequencing (RNA-seq) data, Tang *et al*[11] first screened gene modules partitioned by weighted gene co-expression network analysis that were most relevant to tumor immune phenotype genes. Subsequently, a tumor immune phenotype-related gene signature in liver cancer was identified through least absolute shrinkage and selection operator (LASSO) and univariate Cox regression analyses. Similarly, Wang *et al*[12] employed differential expression analysis and univariate Cox regression to identify differentially expressed genes associated with overall survival. These genes were further refined through LASSO regression to construct a novel immune-related prognostic model in hepatocellular carcinoma. Although bulk RNA-seq provides a global view of gene expression patterns, single-cell RNA-sequencing (scRNA-seq) offers the advantage of revealing heterogeneity within tumors at the single-cell level[10,13]. Therefore, the integration of bulk RNA-seq and scRNA-seq data holds great promise. Yang *et al* [14] utilized scRNA-seq data from liver cancer patients to identify tumor-associated endothelial cell (TEC) subpopulations and established a prognostic model for liver cancer by integrating the marker genes of these cells with bulk RNA-seq data. Li *et al*[15] accurately identified cell subpopulations related to liver cancer by integrating bulk and scRNA-seq data, introducing the cell group structure into the model construction process.

However, cellular crosstalk in the tumor microenvironment should also be considered, as it plays a crucial role in shaping the immune landscape of liver cancer[8,16,17]. The construction of a cell-cell communication network facilitates the identification of key participants in tumor-immune crosstalk. In this context, CellChat, a computational framework for

inferring cell-cell communication, provides a powerful means to identify the communication networks within the liver cancer microenvironment[18,19]. In CellChat, the dynamic process of intercellular communication is simulated using the law of mass action, and the inferred ligand-receptor pairs are systematically classified into functionally relevant signaling pathways[19]. The activity level of a cell group in immune-related pathways can be quantified by counting the number of times the cell group is used as a source and target.

In this study, we aimed to leverage the power of bulk RNA-seq and scRNA-seq data integration to identify a comprehensive immune-related gene signature in liver cancer. By focusing on the cell-cell communication network using the CellChat framework, we sought to unravel the intricate interplay among diverse cell groups within the liver cancer microenvironment. The identified gene signature holds promise for predicting liver cancer prognosis and understanding potential immunotherapeutic responses, providing valuable insights for personalized treatment strategies.

## MATERIALS AND METHODS

### Data collection and preprocessing

The liver cancer bulk RNA-seq data, which included 50 normal and 369 tumor samples, 368 of which included total survival time and status, were downloaded from The Cancer Genome Atlas (TCGA) database. The liver cancer scRNA-seq data were downloaded from the Gene Expression Omnibus database with the accession number GSE125449 and included 8853 cells and 7 cell types[20]: Cancer-associated fibroblast, tumor-associated macrophage, malignant cell, TEC, cells with an unknown entity but that express hepatic progenitor cell markers, T cell, and B cell. For bulk RNA-seq data, a logarithmic transformation with a base of 2 was first performed on the original count data. The expression values of genes with the same name were subsequently averaged. The R package Seurat was used for preprocessing the scRNA-seq data. Specifically, the NormalizeData and FindVariableFeatures functions were used to normalize the data and select 2000 highly variable genes, respectively. Standardization and principal component analysis were performed using the ScaleData and RunPCA functions, respectively. The first ten principal components were used to construct a shared nearest-graph through the FindNeighbors function. Two-dimensional cell visualization was achieved *via* the RunUMAP function.

### Cell-cell communication inference

The Louvain algorithm, employed for cell grouping, was implemented through the function FindClusters in the R package Seurat, with the resolution parameter set to 0.5. Based on these cell grouping results, the cell-cell interaction network was inferred through CellChat. Specifically, the entire human ligand-receptor interaction database CellChatDB was chosen as the foundation for this article. CellChat utilizes the law of mass action to simulate ligand-receptor-mediated signal interactions, which can not only infer intercellular communication but also further classify significant ligand-receptor pairs into functionally related signaling pathways. Immune-related pathways were identified by searching for pathway functions on the official Kyoto Encyclopedia of Genes and Genomes website (<https://www.kegg.jp>). The number of times each cell group served as a source and target in immune-related pathways was counted, and the top 20% of cell groups were considered highly active. Highly active immune-related cells were identified by the intersection of the obtained highly active cell groups with T and B cells.

### LASSO regression and Cox regression

Differential expression analysis was performed through the R package limma[21]. The significantly differentially expressed genes between highly active immune cells and other cells were selected using the criteria  $|\log(\text{fold change})| > 1$  and  $P < 0.05$ . The genes shared between these genes and the bulk RNA-seq data were included in the following LASSO regression model for selecting diagnostic-related features:

$$\min_{w, b} \frac{1}{n} \sum_{i=1}^n (\ln(1 + e^{w^T x_i + b}) - y_i (w^T x_i + b)) + \lambda \| w \|_1 \quad (1)$$

Where  $n$  represents the number of samples,  $w = (w_1, w_2, \dots, w_m)^T$  is the coefficient vector corresponding to  $m$  shared genes,  $x_i = (x_{i1}, x_{i2}, \dots, x_{im})^T$  is the expression level of  $m$  genes in the  $i$ -th sample,  $b$  is the offset,  $\lambda$  represents the regularization parameter determined by 10-fold cross validation, and  $y_i$  represents the label corresponding to the  $i$ -th sample. If a sample was considered to be a tumor, this value was 1; otherwise, it was 0. Eighty percent of the samples were randomly selected as the training set for LASSO regression, while the remaining 20% of the samples were used as the test set to evaluate the effectiveness of the selected diagnostic-related features. The coefficient vector  $w$  and threshold  $b$  in Equation (1) were solved through the R package glmnet[22]. To avoid randomness in the experimental results, the dataset was divided 10 times by setting random seeds from 1 to 10. Genes that were selected more than 5 times were considered diagnostic-related features.

To comprehensively evaluate the impact of risk factors on patient survival, diagnostic-related features were included in the following multivariable Cox regression model:

$$\frac{h(t, x)}{h(t, 0)} = \exp(\beta_1 x_1 + \beta_2 x_2 + \dots + \beta_s x_s) \quad (2)$$

**Table 1** Number of times cell groups served as a source and target in immune-related pathways

| Cell group | Number of times |     |     |    |    |    |    |    |    |    |    |    |    |    |   |
|------------|-----------------|-----|-----|----|----|----|----|----|----|----|----|----|----|----|---|
|            | 12              | 15  | 6   | 2  | 10 | 9  | 14 | 11 | 8  | 1  | 7  | 13 | 3  | 5  | 4 |
| Frequency  | 195             | 195 | 100 | 84 | 76 | 72 | 65 | 50 | 48 | 44 | 41 | 35 | 26 | 22 | 9 |

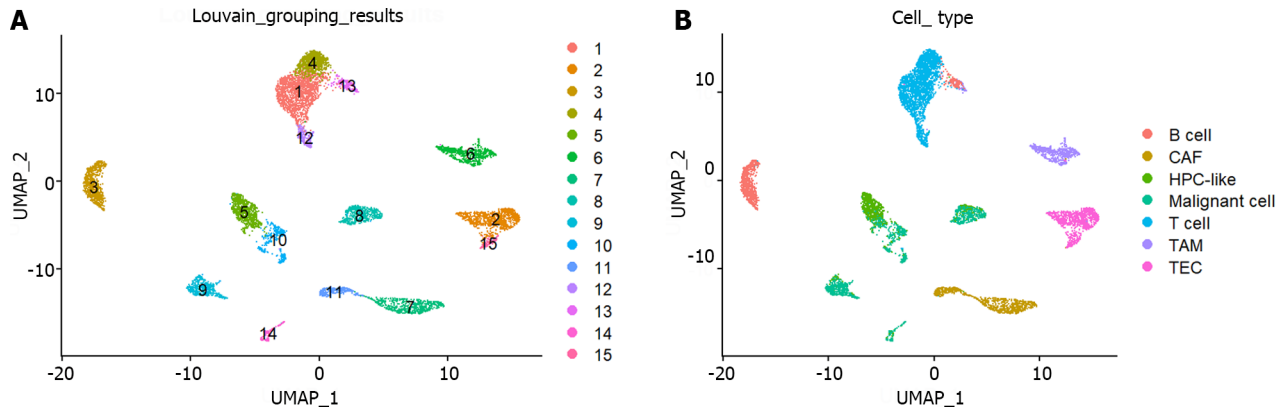


**Figure 1** UMAP visualization of single-cell RNA sequencing data. A: UMAP visualization of 15 cell groups obtained through the Louvain algorithm; B: UMAP visualization of 7 cell types. CAF: Cancer-associated fibroblast; HPC: Hepatic progenitor cell; TAM: Tumor-associated macrophage; TEC: Tumor-associated endothelial cell.

Where  $h(t,x)$  represents the risk function at time  $t$ ,  $h(t,0)$  denotes the baseline risk function, and  $(\beta_1, \beta_2, \dots, \beta_s)^T$  is the regression coefficient vector corresponding to  $s$  diagnostic-related features, which is solved through the R package survival.

**Identification of a gene signature**

After performing multivariable Cox regression analysis, genes significantly associated with survival were selected according to a criterion of  $p < 0.05$  to identify the following gene signature:

$$Risk\ score = \sum_{j=1}^t coef(gene_j) * EXP(gene_j) \tag{3}$$

Where  $gene_j$  represents the  $j$ -th gene among the  $t$  genes significantly associated with survival,  $coef(gene_j)$  represents the coefficient of  $gene_j$  when only genes significantly related to survival were included in the multivariable Cox regression, and  $EXP(gene_j)$  represents the preprocessed expression values of  $gene_j$ . When  $coef(gene_j)$  is greater than 0, the expression level of  $gene_j$  increases, and the patient’s survival risk increases; when the coefficient is less than 0, the expression level of this gene increases, and the survival risk decreases.

**RESULTS**

**Identification of highly active immune cells**

The preprocessed scRNA-seq data were divided into 15 cell groups using the Louvain algorithm. The UMAP visualization of 15 cell groups and 7 cell types was presented in Figure 1A and B, respectively. Subsequently, the communication network between cell groups was inferred through the CellChat, and 16 immune-related pathways were identified. The cell-cell communication within signal pathways inferred integrin beta2 and major histocompatibility class I were demonstrated as examples in Figure 2A and B, respectively. In Figure 2A, cell group 12 serves as the source targeting the other six cell groups, while in Figure 2B, it serves as the target for all cell groups. The number of times each cell group served as a source and target in immune-related pathways was statistically displayed in Table 1. The top 20% of the cell groups in descending order were identified as highly active cell groups, i.e., cell groups 12, 15, and 6. A total of 240 highly active immune cells were identified by intersecting 1009 cells from cell groups 6, 12, and 15 with 3785 T cells and B cells, as shown in Figure 3. These cells are involved in multiple immune-related signaling pathways and play a critical role in regulating immune responses.

**Gene screening and gene signature identification**

Differential expression analysis was also conducted between 240 highly active immune cells and the remaining 8613 cells. Then, 50 significantly differentially expressed genes were identified, and 46 genes shared between them and bulk RNA-

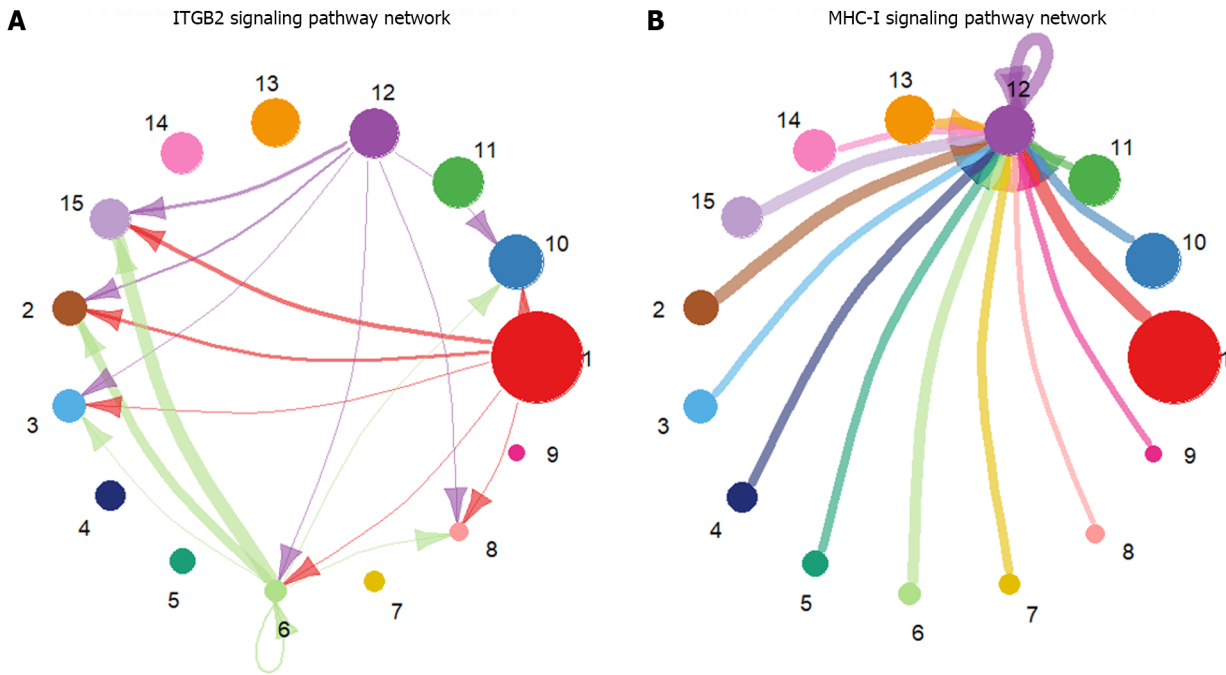


**Figure 2 Circle plot of signaling pathway networks inferred by CellChat.** A: Visualization of the inferred integrin beta2 signaling pathway network details; B: Visualization of the inferred major histocompatibility class I signaling pathway network details. The different colors of the circles represent different cell groups. The size of the circle is proportional to the number of cells in the cell group. The arrows point from the source to the target, and the colors of the edges are consistent with those of the signal source. The width of the edges represents the communication probability. ITGB2: Integrin beta2; MHC-I: Major histocompatibility class I.

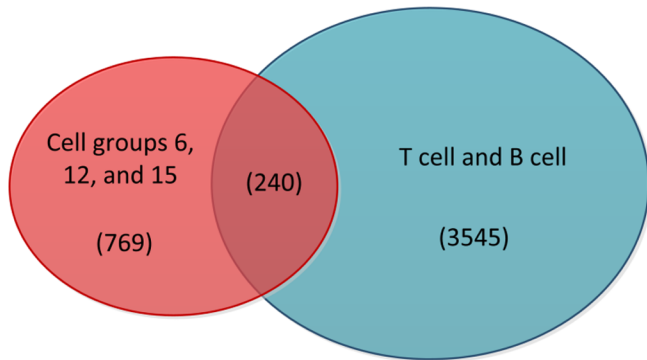


**Figure 3 Venn diagram of highly active cells with T cells and B cells.** The red portion in the diagram represents cells from cell groups 6, 12, and 15, while the blue portion represents T cells and B cells. The middle section indicates the intersection between the two, and the numbers in parentheses correspond to the cell counts in these three sections.

seq data were included in the LASSO regression model. Of these, 14 genes were identified as diagnostic-related genes because they were selected more than 5 times in 10 experiments. The average diagnostic accuracy on the test set over 10 experiments was 96.55%, indicating that the selected features were effective. Subsequently, multivariable Cox regression analysis was conducted, and 3 genes [stathmin 1 (*STMN1*), C-C chemokine ligand 5 (*CCL5*), and cofilin 1 (*CFL1*)] out of 14 were selected to construct a gene signature due to their significant correlation with patient survival. The coefficients and *P* values of the 14 diagnostic-related genes were listed in Table 2. Ultimately, the following gene signature was generated by incorporating only *STMN1*, *CCL5*, and *CFL1* into the multivariable Cox regression analysis model:

$$\text{Risk score} = 0.2754 * \text{EXP}(\text{STMN1}) - 0.2222 * \text{EXP}(\text{CCL5}) + 0.6458 * \text{EXP}(\text{CFL1})$$

Patients with higher risk scores were considered to have worse prognoses. The samples were divided into high-risk and low-risk groups based on the median of this risk score.

**Survival analysis and expression analysis**

To assess the difference in survival between the high-risk and low-risk groups, Kaplan-Meier survival analysis was conducted, and the log-rank test was employed for statistical analysis. Figure 4 illustrated the significant difference between the high-risk and low-risk groups (*P* < 0.0001), with the median survival time of patients in the low-risk group being approximately three times longer than that in the high-risk group. These results indicated that the identified gene

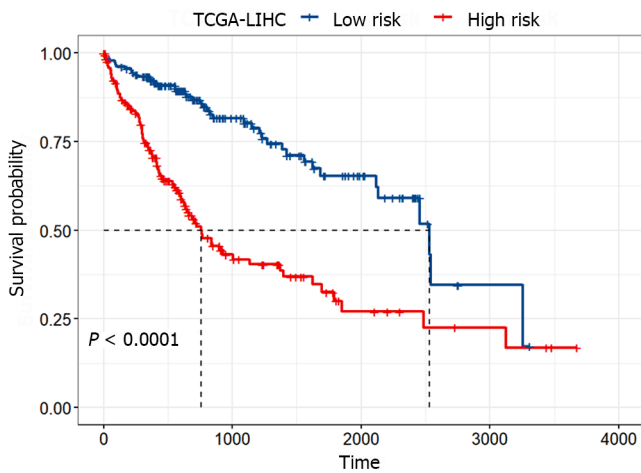


**Figure 4 Kaplan-Meier survival curves of the high-risk and low-risk groups.** The red and blue curves represent the high-risk and low-risk groups, respectively, which were divided according to the median risk score. The significance of the difference between the two was evaluated through the log-rank test. TCGA-LIHC: The Cancer Genome Atlas Liver Hepatocellular Carcinoma.

signature could significantly distinguish between patients with favorable and poor prognoses.

Furthermore, expression analysis of the individual genes constituting the gene signature was conducted in the high-risk and low-risk groups, as well as in tumor and normal samples; the results were presented in Figure 5. A *t* test was performed to assess whether there were significant differences between two groups of samples, and the obtained *P* values were displayed in all boxplots. The *STMN1* and *CFL1* genes had significantly greater expression in the high-risk group and tumor samples, while the *CCL5* gene had greater expression in the low-risk group and normal samples. Meta-analysis revealed that in liver cancer, *STMN1* and *CFL1* are considered oncogenes, and their upregulation is closely associated with poor prognosis[23,24]. The *CCL5*-high subtype is significantly correlated with immune cells and markedly improved overall survival[25]. This finding is consistent with the findings in Figure 5, providing additional confirmation for the reliability of the identified gene signature.

### Immunocyte infiltration analysis

The relative infiltration of immune cells in the high-risk and low-risk groups was investigated using the single-sample gene set enrichment analysis algorithm[26]. This algorithm was implemented through the function GSVA in the R package GSVA. A reference gene set comprising 28 reported immune cell types was utilized for the analysis[27]. Figure 6 showed that out of the 28 immune cell types, 20 exhibited significant correlations with the risk groups. The Kruskal-Wallis test was used to evaluate significant differences between two groups. In particular, the infiltration levels in cell types activated B cell, effector memory CD8 T cell, eosinophil, immature B cell, mast cell, and type 1 T helper cell were significantly greater in the low-risk group than in the high-risk group. These results indicated that an immune-related gene signature identified through cell-cell communication plays a crucial role in stratifying the risk of liver cancer.

### Tumor mutation burden analysis

Tumor mutation burden (TMB) was approved by the United States Food and Drug Administration in 2020 as a biomarker for predicting the response to immunotherapy[28]. To assess the relationship between the identified gene signature and the immune response, the TMB of the samples was computed using mutation data obtained from liver cancer patients downloaded from the TCGA database. Figure 7A illustrated the TMB distribution across all samples. Figure 7B and C showed the mutation landscapes of the high-risk and the low-risk groups, respectively. Among the top 10 mutated genes, 6 were common between the high-risk group and the low-risk group, but each gene had a different mutation type. Furthermore, the TMB in the high-risk and low-risk groups identified by the gene signature proposed in this article, as well as the groups identified by the gene signatures proposed by Tang *et al*[11] and Wang *et al*[12], were separately analyzed, as shown in Figure 7D-F. However, only the samples from the high-risk and low-risk groups defined by the proposed gene signature showed a significant difference in TMB ( $P = 0.01106$ ). These results strongly demonstrated that the identified gene signature could predict the efficacy of immunotherapy.

### Prediction of immunotherapy response

The TIDE algorithm, which simulates both the immune evasion mechanisms of immune function suppression and immune cell exclusion, more accurately predicts patient prognosis than individual biomarkers alone[29]. Currently, this algorithm has been widely applied for predicting patient responses to ICB therapy. In this article, the TIDE algorithm was used to analyze the response of liver cancer patients to immunotherapy using an online tool (<http://tide.dfci.harvard.edu/>). A higher TIDE score indicates that the patient is more prone to experiencing immune escape and is likely to exhibit poor efficacy in response to immunotherapy. The Pearson correlation coefficient between TIDE scores and Risks cores was calculated, and the significant correlation trends between the two were illustrated in Figure 8A.

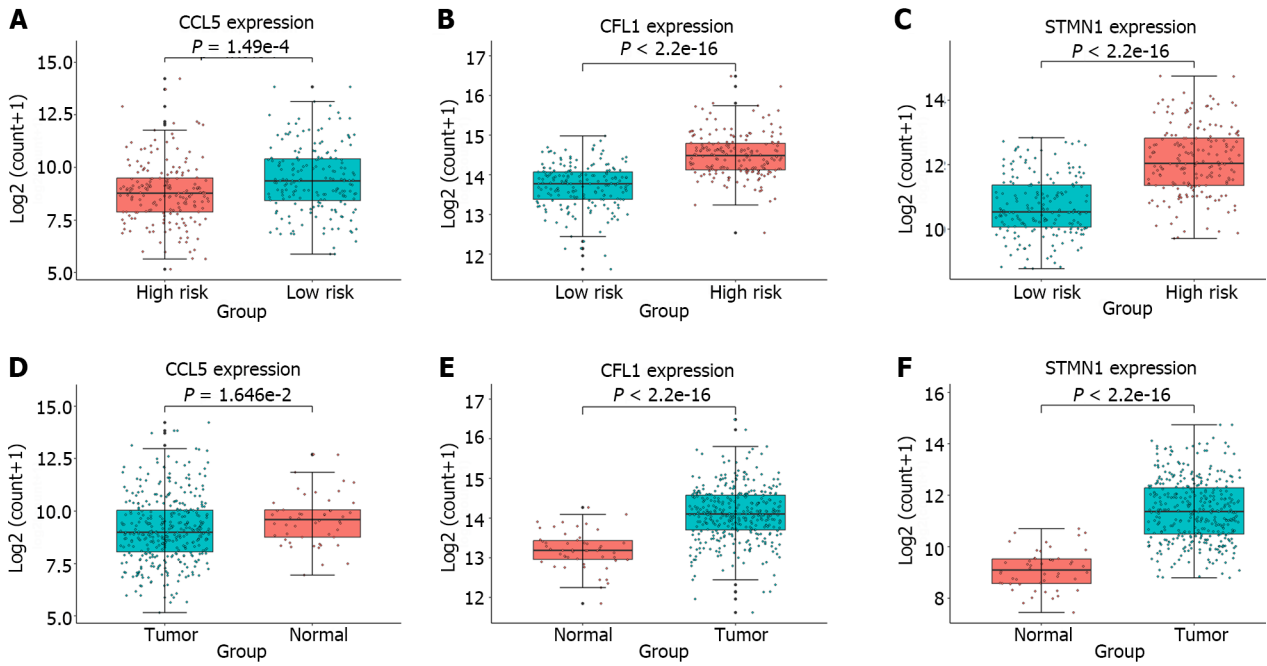


**Figure 5** Box plots depicting the expression analysis of the genes employed in constructing the gene signature. A-C: Expression analysis of C-C chemokine ligand 5 (CCL5), cofilin 1 (CFL1), and stathmin 1 (STMN1) in the high-risk and low-risk groups; D-F: Expression analysis of CCL5, CFL1, and STMN1 in the tumor and normal groups. The high-risk and normal groups are represented by red boxes, while the low-risk and tumor groups are represented by blue boxes. The significant differences between groups were evaluated through t tests. CCL5: C-C chemokine ligand 5; CFL1: Cofilin 1; STMN1: Stathmin 1.

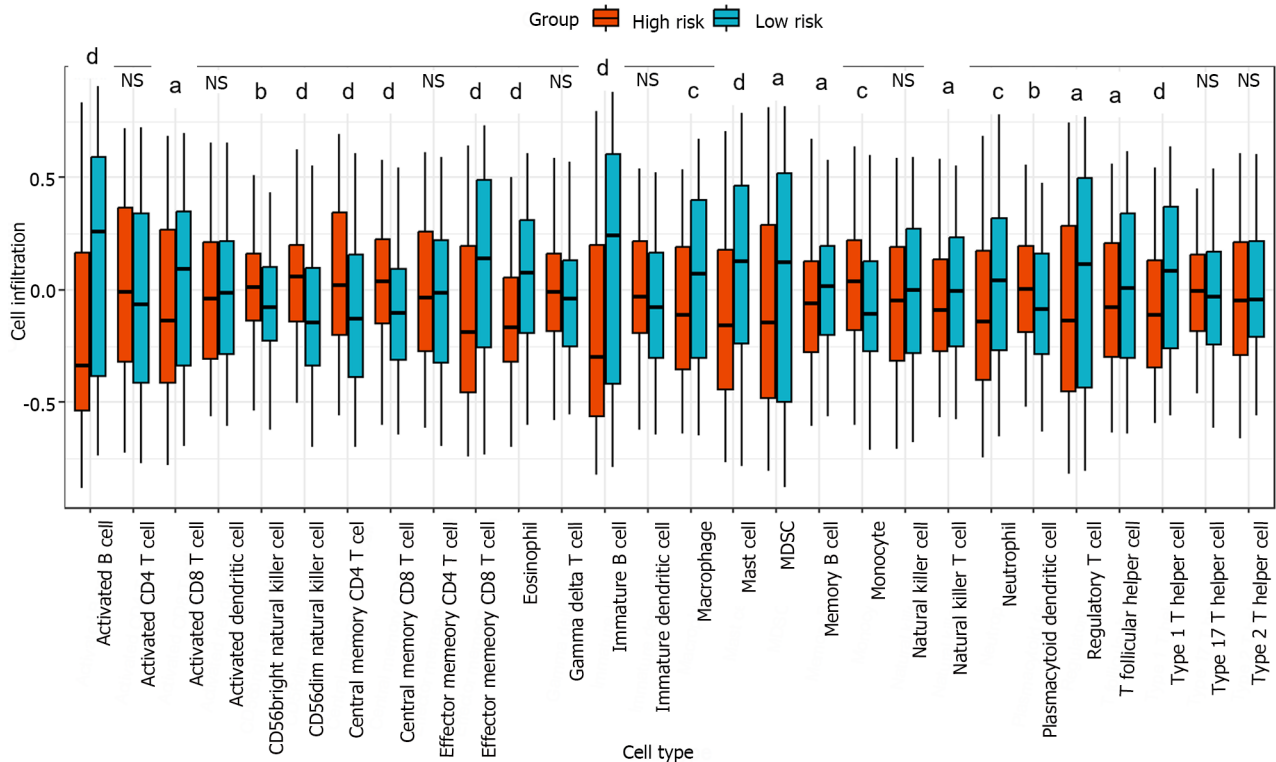


**Figure 6** Box plot of the degree of immune cell infiltration in the high-risk and low-risk groups. The infiltration degree of 28 immune cell types in the high-risk and low-risk groups was analyzed, and the significant differences between the two groups were evaluated using the Kruskal-Wallis test. <sup>a</sup> $P < 0.05$ ; <sup>b</sup> $P < 0.01$ ; <sup>c</sup> $P < 0.001$ ; <sup>d</sup> $P < 0.0001$ .

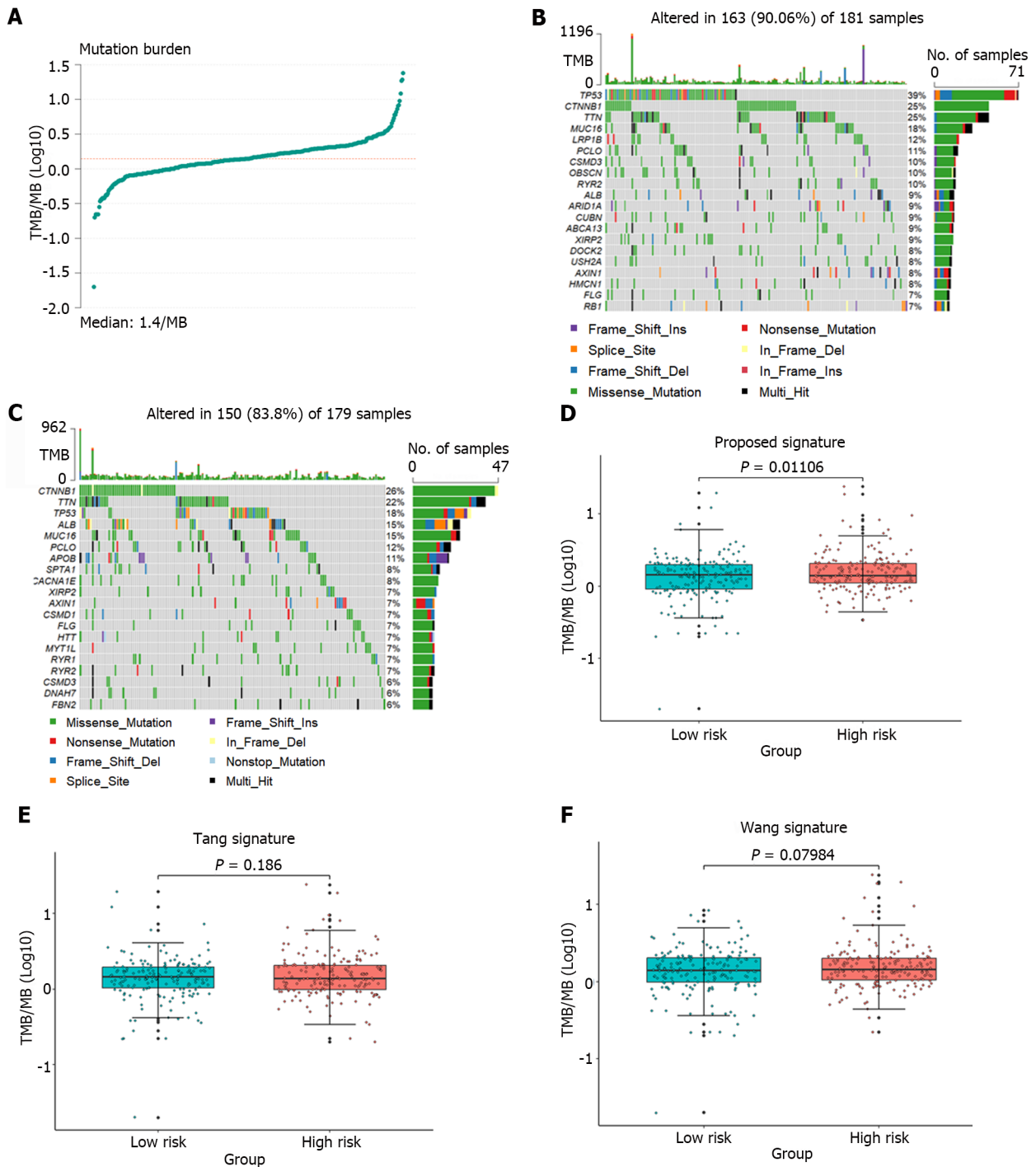


**Figure 7 Analysis of the tumor mutation burden in the samples.** A: The distribution of tumor mutation burden (TMB) for all samples; B and C: Waterfall plots depicting mutation landscapes in the high-risk and low-risk groups, respectively; D-F: A comparative analysis of TMB was conducted in the high-risk and low-risk groups identified by the gene signature identified in this article and the groups identified by the gene signature proposed by Tang *et al*[11] and Wang *et al*[12].

Furthermore, the TIDE scores corresponding to the high-risk and low-risk groups identified by the gene signature in this article, as well as the groups identified by the gene signatures reported by Tang *et al*[11] and Wang *et al*[12], are depicted in Figure 8B-D. The TIDE scores exhibited significant differences across all high-risk and low-risk groups, with the minimum  $P$  value observed among groups stratified by the proposed gene signature ( $P = 3.762e-10$ ). Moreover, compared to those of the other two methods, the gene signature identified in this article requires the fewest genes. A significant correlation was observed between TIDE score and Risk scores, and a distinction was made between the high-risk and low-risk groups, suggesting that the identified gene signature could serve as a valuable tool for predicting the efficacy of immunotherapy.

**Table 2** Coefficients and *P* values corresponding to diagnostic-related genes in multivariable Cox regression

| Gene   | Coefficient  | <i>P</i> value |
|--------|--------------|----------------|
| NUSAP1 | -0.108515073 | 0.219706452    |
| STMN1  | 0.367886836  | 0.006598885    |
| UBE2C  | -0.038808062 | 0.692223045    |
| CKS1B  | 0.019614361  | 0.885123337    |
| HMGB1  | -0.036928764 | 0.841313659    |
| CCL5   | -0.351813314 | 0.000909645    |
| DUT    | -0.200404711 | 0.201189097    |
| PFN1   | 0.156824573  | 0.389822262    |
| ITM2A  | -0.021567354 | 0.742760958    |
| CCL4   | 0.146793282  | 0.182629575    |
| CFL1   | 0.688652826  | 0.001683044    |
| IL32   | -0.054741614 | 0.491028415    |
| MT2A   | 0.033545401  | 0.525093809    |
| IFITM3 | -0.053229362 | 0.706251853    |

NUSAP1: Nucleolar and spindle associated protein 1; STMN1: Stathmin 1; UBE2C: Ubiquitin conjugating enzyme E2 C; CKS1B: CDC28 protein kinase regulatory subunit 1B; HMGB1: High mobility group box 1; CCL5: C-C chemokine ligand 5; DUT: Deoxyuridine triphosphatase; PFN1: Profilin 1; ITM2A: Integral membrane protein 2A; CCL4: C-C chemokine ligand 4; CFL1: Cofilin 1; IL32: Interleukin 32; MT2A: Metallothionein 2A; IFITM3: Interferon induced transmembrane protein 3.

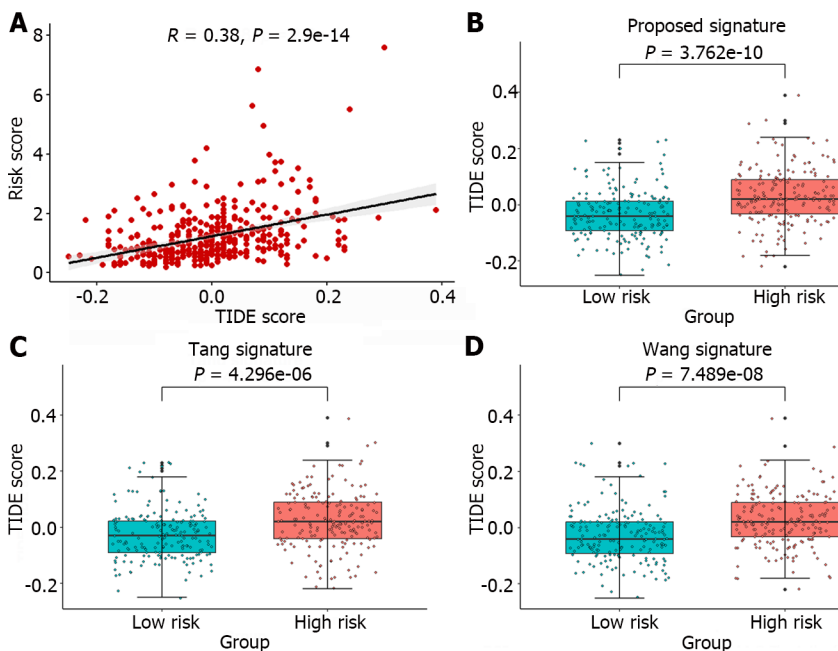


**Figure 8** Analysis of predicted TIDE scores in the sample. A: Pearson correlation analysis between the sample risk score and TIDE score; B-D: A comparative analysis of the TIDE score was conducted for the high-risk and low-risk groups identified by the gene signature in this article and the groups identified by the gene signatures proposed by Tang *et al*[11] and Wang *et al*[12].

## DISCUSSION

Our research demonstrated that utilizing cell-cell communication information to identify immune-related gene signature outperformed two other methods in terms of predictive performance. However, it's worth noting that we focused on cell-cell communication at the cell group level rather than at the level of individual cells. Investigating the interactions between cells at single-cell resolution and their impact on predicting patient prognosis and immunotherapeutic efficacy is

a direction for our future research.

---

## CONCLUSION

---

In summary, our integrated analysis of bulk and scRNA-seq data, coupled with the exploration of the cell-cell communication network, has identified a comprehensive immune-related gene signature with clinical and therapeutic implications. The identified gene signature not only demonstrates potential as a prognostic tool for liver cancer but also provides invaluable insights into the dynamics of immune responses within the tumor microenvironment.

## ARTICLE HIGHLIGHTS

### **Research background**

Immunotherapy has provided hope to patients with advanced liver cancer, but only a small fraction of patients benefit from this treatment due to individual differences. Although several methods have been developed to predict the prognosis and immunotherapeutic efficacy in patients with liver cancer, the impact of cell-cell interactions in the tumor microenvironment has not been adequately considered.

### **Research motivation**

Recent research has demonstrated the crucial role of cell-cell interactions in shaping the immune landscape of liver cancer.

### **Research objectives**

This study aims to identify immune-related gene signatures through cell-cell interactions to predict prognosis and immunotherapeutic efficacy in liver cancer.

### **Research methods**

In this study, CellChat was employed to infer cell-cell communication, thereby selecting highly active cell groups in immune-related pathways on single-cell RNA-sequencing (scRNA-seq) data. Highly active immune cells were identified by intersecting these groups with B and T cells. Subsequently, significantly differentially expressed genes between highly active immune cells and the remaining cells were incorporated into the Lasso regression model. Ultimately, incorporating genes selected more than 5 times in 10 Lasso regression experiments into a multivariable Cox regression model, 3 genes (stathmin 1, cofilin 1, and C-C chemokine ligand 5) significantly associated with survival were identified to construct a gene signature.

### **Research results**

The immune-related gene signature composed of stathmin 1, cofilin 1, and C-C chemokine ligand 5 was identified through cell-cell communication. The identified gene signature has been validated to be superior to the other two methods through immunotherapy response prediction, tumor mutation burden analysis, and immune cell infiltration analysis, enabling better prediction of prognosis and immune therapy efficacy in liver cancer.

### **Research conclusions**

This study suggests that the identified gene signature may contribute to a deeper understanding of the activity patterns of immune cells in the liver tumor microenvironment, providing insights for personalized treatment strategies.

### **Research perspectives**

This article utilized cell-cell communication information and machine learning method, combined with Cox regression, to comprehensively analyze bulk and scRNA-seq data, identifying clinically and therapeutically relevant immune-related gene signature.

---

## FOOTNOTES

---

**Co-corresponding authors:** Hong-Mei Zhang and Dong-Qing Wei.

**Author contributions:** Zhang HM and Wei DQ contributed equally to this work and should be considered co-corresponding authors. Li JT and Zhang HM conceived this study and implemented the experiments; Li JT and Wang W collected and preprocessed the data; Zhang HM and Wei DQ drafted and revised the manuscript.

**Supported by** Scientific and Technological Project of Henan Province, No. 212102210140.

**Institutional review board statement:** This study doesn't involve any human subjects.

**Conflict-of-interest statement:** All the authors report no relevant conflicts of interest for this article.

**Open-Access:** This article is an open-access article that was selected by an in-house editor and fully peer-reviewed by external reviewers. It is distributed in accordance with the Creative Commons Attribution NonCommercial (CC BY-NC 4.0) license, which permits others to distribute, remix, adapt, build upon this work non-commercially, and license their derivative works on different terms, provided the original work is properly cited and the use is non-commercial. See: <https://creativecommons.org/licenses/by-nc/4.0/>

**Country/Territory of origin:** China

**ORCID number:** Jun-Tao Li 0000-0002-3288-4395; Hong-Mei Zhang 0009-0003-0914-1539; Wei Wang 0000-0002-9616-1145; Dong-Qing Wei 0000-0003-4200-7502.

**S-Editor:** Wang JJ

**L-Editor:** A

**P-Editor:** Cai YX

## REFERENCES

- Sung H, Ferlay J, Siegel RL, Laversanne M, Soerjomataram I, Jemal A, Bray F. Global Cancer Statistics 2020: GLOBOCAN Estimates of Incidence and Mortality Worldwide for 36 Cancers in 185 Countries. *CA Cancer J Clin* 2021; **71**: 209-249 [PMID: 33538338 DOI: 10.3322/caac.21660]
- Bakrania A, Joshi N, Zhao X, Zheng G, Bhat M. Artificial intelligence in liver cancers: Decoding the impact of machine learning models in clinical diagnosis of primary liver cancers and liver cancer metastases. *Pharmacol Res* 2023; **189**: 106706 [PMID: 36813095 DOI: 10.1016/j.phrs.2023.106706]
- Villarruel-Melquiades F, Mendoza-Garrido ME, García-Cuellar CM, Sánchez-Pérez Y, Pérez-Carreón JI, Camacho J. Current and novel approaches in the pharmacological treatment of hepatocellular carcinoma. *World J Gastroenterol* 2023; **29**: 2571-2599 [PMID: 37213397 DOI: 10.3748/wjg.v29.i17.2571]
- Fritz JM, Lenardo MJ. Development of immune checkpoint therapy for cancer. *J Exp Med* 2019; **216**: 1244-1254 [PMID: 31068379 DOI: 10.1084/jem.20182395]
- Kalbasi A, Ribas A. Tumour-intrinsic resistance to immune checkpoint blockade. *Nat Rev Immunol* 2020; **20**: 25-39 [PMID: 31570880 DOI: 10.1038/s41577-019-0218-4]
- Shen W, Chen Y, Lei P, Sheldon M, Sun Y, Yao F, Ma L. Immunotherapeutic Approaches for Treating Hepatocellular Carcinoma. *Cancers (Basel)* 2022; **14** [PMID: 36291797 DOI: 10.3390/cancers14205013]
- Llovet JM, Castet F, Heikenwalder M, Maini MK, Mazzaferro V, Pinato DJ, Pikarsky E, Zhu AX, Finn RS. Immunotherapies for hepatocellular carcinoma. *Nat Rev Clin Oncol* 2022; **19**: 151-172 [PMID: 34764464 DOI: 10.1038/s41571-021-00573-2]
- Donne R, Lujambio A. The liver cancer immune microenvironment: Therapeutic implications for hepatocellular carcinoma. *Hepatology* 2023; **77**: 1773-1796 [PMID: 35989535 DOI: 10.1002/hep.32740]
- Thorgeirsson SS, Lee JS, Grisham JW. Molecular prognostication of liver cancer: end of the beginning. *J Hepatol* 2006; **44**: 798-805 [PMID: 16488507 DOI: 10.1016/j.jhep.2006.01.008]
- Suvà ML, Tirosch I. Single-Cell RNA Sequencing in Cancer: Lessons Learned and Emerging Challenges. *Mol Cell* 2019; **75**: 7-12 [PMID: 31299208 DOI: 10.1016/j.molcel.2019.05.003]
- Tang Y, Guo C, Yang Z, Wang Y, Zhang Y, Wang D. Identification of a Tumor Immunological Phenotype-Related Gene Signature for Predicting Prognosis, Immunotherapy Efficacy, and Drug Candidates in Hepatocellular Carcinoma. *Front Immunol* 2022; **13**: 862527 [PMID: 35493471 DOI: 10.3389/fimmu.2022.862527]
- Wang Z, Zhu J, Liu Y, Liu C, Wang W, Chen F, Ma L. Development and validation of a novel immune-related prognostic model in hepatocellular carcinoma. *J Transl Med* 2020; **18**: 67 [PMID: 32046766 DOI: 10.1186/s12967-020-02255-6]
- Yofe I, Dahan R, Amit I. Single-cell genomic approaches for developing the next generation of immunotherapies. *Nat Med* 2020; **26**: 171-177 [PMID: 32015555 DOI: 10.1038/s41591-019-0736-4]
- Yang D, Kuang T, Zhou Y, Su Y, Shen J, Yu B, Zhao K, Ding Y. Tumor-associated endothelial cell prognostic risk model and tumor immune environment modulation in liver cancer based on single-cell and bulk RNA sequencing: Experimental verification. *Int Immunopharmacol* 2023; **124**: 110870 [PMID: 37690233 DOI: 10.1016/j.intimp.2023.110870]
- Li J, Zhang H, Mu B, Zuo H, Zhou K. Identifying phenotype-associated subpopulations through LP\_SGL. *Brief Bioinform* 2023; **25** [PMID: 38008419 DOI: 10.1093/bib/bbad424]
- Zhou G, Boor PPC, Bruno MJ, Sprengers D, Kwekkeboom J. Immune suppressive checkpoint interactions in the tumour microenvironment of primary liver cancers. *Br J Cancer* 2022; **126**: 10-23 [PMID: 34400801 DOI: 10.1038/s41416-021-01453-3]
- Zhang Q, Lou Y, Bai XL, Liang TB. Immunometabolism: A novel perspective of liver cancer microenvironment and its influence on tumor progression. *World J Gastroenterol* 2018; **24**: 3500-3512 [PMID: 30131656 DOI: 10.3748/wjg.v24.i31.3500]
- Ma L, Heinrich S, Wang L, Keggenhoff FL, Khatib S, Forgues M, Kelly M, Hewitt SM, Saif A, Hernandez JM, Mabry D, Kloeckner R, Greten TF, Chaisaingmongkol J, Ruchirawat M, Marquardt JU, Wang XW. Multiregional single-cell dissection of tumor and immune cells reveals stable lock-and-key features in liver cancer. *Nat Commun* 2022; **13**: 7533 [PMID: 36476645 DOI: 10.1038/s41467-022-35291-5]
- Jin S, Guerrero-Juarez CF, Zhang L, Chang I, Ramos R, Kuan CH, Myung P, Plikus MV, Nie Q. Inference and analysis of cell-cell communication using CellChat. *Nat Commun* 2021; **12**: 1088 [PMID: 33597522 DOI: 10.1038/s41467-021-21246-9]
- Ma L, Hernandez MO, Zhao Y, Mehta M, Tran B, Kelly M, Rae Z, Hernandez JM, Davis JL, Martin SP, Kleiner DE, Hewitt SM, Ylaja K, Wood BJ, Greten TF, Wang XW. Tumor Cell Biodiversity Drives Microenvironmental Reprogramming in Liver Cancer. *Cancer Cell* 2019; **36**: 418-430.e6 [PMID: 31588021 DOI: 10.1016/j.ccell.2019.08.007]
- Ritchie ME, Phipson B, Wu D, Hu Y, Law CW, Shi W, Smyth GK. limma powers differential expression analyses for RNA-sequencing and

- microarray studies. *Nucleic Acids Res* 2015; **43**: e47 [PMID: 25605792 DOI: 10.1093/nar/gkv007]
- 22 **Friedman J**, Hastie T, Tibshirani R. Regularization Paths for Generalized Linear Models via Coordinate Descent. *J Stat Softw* 2010; **33**: 1-22 [PMID: 20808728 DOI: 10.18637/jss.v033.i01]
- 23 **Zhang R**, Gao X, Zuo J, Hu B, Yang J, Zhao J, Chen J. STMN1 upregulation mediates hepatocellular carcinoma and hepatic stellate cell crosstalk to aggravate cancer by triggering the MET pathway. *Cancer Sci* 2020; **111**: 406-417 [PMID: 31785057 DOI: 10.1111/cas.14262]
- 24 **Li S**, Xu L, Wu G, Huang Z, Huang L, Zhang F, Wei C, Shen Q, Li R, Zhang L, Xu X. Remodeling Serine Synthesis and Metabolism via Nanoparticles (NPs)-Mediated CFL1 Silencing to Enhance the Sensitivity of Hepatocellular Carcinoma to Sorafenib. *Adv Sci (Weinh)* 2023; **10**: e2207118 [PMID: 37203277 DOI: 10.1002/advs.202207118]
- 25 **Xia Y**, Zhou L, Yang HC, Yu CW. Chemokine CCL5 immune subtypes of human liver cancer with prognostic significance. *Int Immunopharmacol* 2022; **113**: 109372 [PMID: 36332449 DOI: 10.1016/j.intimp.2022.109372]
- 26 **Barbie DA**, Tamayo P, Boehm JS, Kim SY, Moody SE, Dunn IF, Schinzel AC, Sandy P, Meylan E, Scholl C, Fröhling S, Chan EM, Sos ML, Michel K, Mermel C, Silver SJ, Weir BA, Reiling JH, Sheng Q, Gupta PB, Wadlow RC, Le H, Hoersch S, Wittner BS, Ramaswamy S, Livingston DM, Sabatini DM, Meyerson M, Thomas RK, Lander ES, Mesirov JP, Root DE, Gilliland DG, Jacks T, Hahn WC. Systematic RNA interference reveals that oncogenic KRAS-driven cancers require TBK1. *Nature* 2009; **462**: 108-112 [PMID: 19847166 DOI: 10.1038/nature08460]
- 27 **Charoentong P**, Finotello F, Angelova M, Mayer C, Efremova M, Rieder D, Hackl H, Trajanoski Z. Pan-cancer Immunogenomic Analyses Reveal Genotype-Immunophenotype Relationships and Predictors of Response to Checkpoint Blockade. *Cell Rep* 2017; **18**: 248-262 [PMID: 28052254 DOI: 10.1016/j.celrep.2016.12.019]
- 28 **Subbiah V**, Solit DB, Chan TA, Kurzrock R. The FDA approval of pembrolizumab for adult and pediatric patients with tumor mutational burden (TMB)  $\geq 10$ : a decision centered on empowering patients and their physicians. *Ann Oncol* 2020; **31**: 1115-1118 [PMID: 32771306 DOI: 10.1016/j.annonc.2020.07.002]
- 29 **Jiang P**, Gu S, Pan D, Fu J, Sahu A, Hu X, Li Z, Traugh N, Bu X, Li B, Liu J, Freeman GJ, Brown MA, Wucherpfennig KW, Liu XS. Signatures of T cell dysfunction and exclusion predict cancer immunotherapy response. *Nat Med* 2018; **24**: 1550-1558 [PMID: 30127393 DOI: 10.1038/s41591-018-0136-1]



Published by **Baishideng Publishing Group Inc**  
7041 Koll Center Parkway, Suite 160, Pleasanton, CA 94566, USA  
**Telephone:** +1-925-3991568  
**E-mail:** [office@baishideng.com](mailto:office@baishideng.com)  
**Help Desk:** <https://www.f6publishing.com/helpdesk>  
<https://www.wjgnet.com>

